Fast Determination of Regional Myocardial Strain Fields From Tagged Cardiac Images Using Harmonic Phase MRI

Jérôme Garot, MD; David A. Bluemke, MD, PhD; Nael F. Osman, PhD; Carlos E. Rochitte, MD; Elliot R. McVeigh, PhD; Elias A. Zerhouni, MD; Jerry L. Prince, PhD; João A.C. Lima, MD

Background—Tagged MRI of the heart is difficult to implement clinically because of the lack of fast analytical techniques. We investigated the accuracy of harmonic phase (HARP) imaging for rapid quantification of myocardial strains and for detailed analysis of left ventricular (LV) function during dobutamine stimulation.

Methods and Results—Tagged MRI was performed in 10 volunteers at rest and during 5 to 20 $\mu g^{-1} \cdot kg^{-1} \cdot min^{-1}$ dobutamine and in 9 postinfarct patients at rest. We compared 2D myocardial strains (circumferential shortening, Ecc; maximal shortening, E_2; and E_2, direction) as assessed by a conventional technique and by HARP. Full quantitative analysis of the data was 10 times faster with HARP. For pooled data, the regression coefficient was $r=0.93$ for each strain ($P<0.001$). In volunteers, Ecc and E_2 were greater in the free wall than in the septum ($P<0.01$), but recruitable myocardial strain at peak dobutamine was greater in the LV septum ($P<0.01$). E_2 orientation shifted away from the circumferential direction at peak dobutamine ($P<0.01$). HARP accurately detected subtle changes in myocardial strain fields under increasing doses of dobutamine. In patients, HARP-determined Ecc and E_2 values were dramatically reduced in the asynergic segments as compared with remote ($P<0.001$), and E_2 direction shifted away from the circumferential direction ($P<0.001$).

Conclusions—HARP MRI provides fast, accurate assessment of myocardial strains from tagged MR images in normal subjects and in patients with coronary artery disease with wall motion abnormalities. HARP correctly indexes dobutamine-induced changes in strains and has the potential for on-line quantitative monitoring of LV function during stress testing. **(*Circulation*. 2000;101:981-988.)**

Key Words: magnetic resonance imaging ■ ventricles ■ myocardium ■ contractility

The analyses of myocardial wall motion abnormalities with dobutamine stress echocardiography[1] and MRI[2] are established methods for the detection of myocardial ischemia. However, the assessment of regional left ventricular (LV) function by either method is semiquantitative and subjective.[2,3] Tagged MRI of the heart is a valuable technique for the quantitative noninvasive assessment of regional myocardial contractile performance.[4–6] The spatial modulation of magnetization (SPAMM) technique generates 2 orthogonal sets of parallel planes of magnetic saturation by a sequence of nonselective radiofrequency pulses.[7,8] The myocardium appears with a spatially encoded pattern that moves with the tissue and can be analyzed to reconstruct myocardial motion. Several methods for reconstructing LV strain fields have been proposed.[5,6,9,10] The position of the tags must be measured with the use of a tag detection algorithm[11] and myocardial motion computed from displacement information from each tag.[12,13] However, the process is time consuming because it requires the tracking of tag lines and myocardial contours with an interactive computer-aided technique.[11,13] The lack of fast analytical techniques of myocardial strain quantification represents the main limitation to routine clinical utilization of tagged cardiac MRI.

SPAMM-tagged MR images correspond to a collection of spectral peaks in the Fourier domain.[7,8] The inverse Fourier transform of one of these peaks is a complex image whose phase is linearly related to a directional component of the tissue displacement. A harmonic phase (HARP) image is the calculated phase of this complex image, which can be used to synthesize conventional tag lines and calculate 2D myocardial strain.[14] This HARP imaging approach[14] allows fast visualization and automated analysis of tagged cardiac MR images. Its potential in clinical cardiology depends on the demonstration of its sensitivity to small changes in myocardial strain during pharmacological stress testing and on its ability to accurately index regional wall motion abnormalities. We investigated the accuracy of HARP for quantitative assessment of 2D myocardial strain fields in normal individ-

Received July 28, 1999; revision received September 20, 1999; accepted October 6, 1999.

From the Cardiology Division of the Department of Medicine (J.G., C.E.R., J.A.C.L.) and the Departments of Radiology (D.A.B., E.A.Z.) and Biomedical Engineering (E.R.M.) of the Johns Hopkins University School of Medicine, and the Department of Electrical and Computer Engineering of the Whiting School of Engineering (N.F.O., J.L.P.), Johns Hopkins University, Baltimore, Md.

Correspondence to João A.C. Lima, MD, Cardiology Division, Blalock 569, Johns Hopkins Hospital, 600 N Wolfe St, Baltimore, MD 21287-6568. E-mail jlima@welchlink.welch.jhu.edu

Circulation **is available at http://www.circulationaha.org**

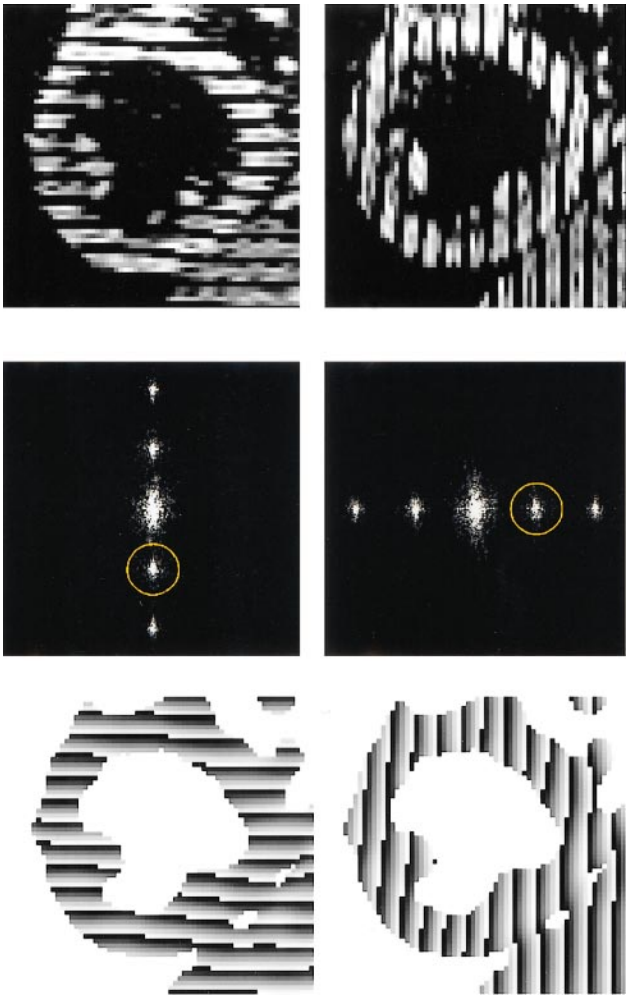

Figure 1. SPAMM-tagged images of the LV short-axis view (top), the magnitudes of the corresponding Fourier transform (middle), and the corresponding HARP images (bottom). Circles in the Fourier domain correspond to the size of the bandpass filter.

uals who underwent dobutamine stress–tagged MRI and in postinfarct patients with underlying abnormal regional LV function.

Methods

Study Population

SPAMM-tagged MR images were obtained in the short-axis view under a dobutamine challenge in 10 healthy male volunteers (age 37±10 years). All volunteers had no history of chest pain, prior cardiovascular disease, or cardiovascular risk factors. We also studied 9 patients at baseline (8 men, age 43±11 years) 3±2 days after a first acute myocardial infarction (AMI, 4 anterior, 5 inferior). Informed written consent was obtained according to the standards of the Joint Committee for Clinical Investigation of the Johns Hopkins Hospital.

MRI Protocol

Images were acquired during multiple breath-holds on a 1.5-T whole-body magnet (Signa, General Electric Medical Systems). Anterior and posterior phased-array coils were used for signal acquisition. We used an ECG-triggered segmented k-space fast gradient-echo imaging pulse sequence.[15] The tagging pulse sequence consisted of nonselective radiofrequency pulses separated by spatial modulation of magnetization-encoding gradients to achieve tag separation of 7 mm. After scout images were completed, contiguous stacks of 4 base-to-apex short-axis cross sections were prescribed. Two sets of identical short-axis views were acquired (the second set rotated by 90°). A slab saturation band was applied to presaturate the blood in the LV, resulting in "black blood" in the LV cavity. This imaging sequence allowed us to image 4 slices within 4 breath-holds (≈14 to 20 seconds each). The number of views per phase was decreased as heart rate increased to maximize temporal resolution. Scanner settings were field of view 36 cm, tag separation 7 mm, slice thickness 8 mm, TR 6.5 ms, TE 2.3 ms, tip angle 15°, and image matrix 256×160, with 5 to 7 phase-encoded views per movie frame and cardiac cycle.

Dobutamine Stress–MR study

A single-lead ECG was continuously monitored and blood pressure was recorded at baseline and every 3 minutes throughout the procedure. After baseline acquisitions, dobutamine was infused through a digital infusion pump at 5 and 20 $\mu g^{-1} \cdot kg^{-1} \cdot min^{-1}$. Imaging began 2 minutes after each dose increase and required 3 minutes for each of the 4 levels. Criteria for terminating the study were (1) acceleration of heart rate >100% of age-predicted maximal heart rate, (2) fall of systolic blood pressure >30 mm Hg, (3) chest pain compatible with angina, (4) frequent ventricular or supraventricular ectopic beats, (5) intolerable side effects of dobutamine.

Harmonic Phase Imaging

The SPAMM technique uses a special pulse sequence to spatially modulate the longitudinal magnetization of the myocardium before acquiring image data.[7,8] SPAMM-tagged images have regularly distributed spectral peaks in k-space, and each peak contains information about tag motion in a given direction. HARP imaging is based on the use of isolated peaks extracted with a bandpass filter (Figure 1) (Appendix A). One spectral peak was extracted for each direction of tag lines.[14] The inverse Fourier transform of one of these peaks is a complex image whose phase is linearly related to a directional component of the true motion. The principal value of the phase was used to construct a HARP image (Figure 1) (Appendix A), which is linearly related to a component of the 3D motion except that it is constrained to lie in the range $(-\pi, +\pi)$. Slopes of phases reflect the frequency of the tag pattern and phase images reflect motion of the heart. HARP images can be used to measure 2D strains[14,16] (Appendix B), described as normalized myocardial deformation in a specific direction given by a unit vector. Figure 2 shows examples of 2D strain maps of the LV short-axis view throughout systole in a healthy volunteer at 5 and 20 $\mu g^{-1} \cdot kg^{-1} \cdot min^{-1}$ dobutamine.

Strain Computation by Operator-Controlled Segmentation

Myocardial strains were assessed off-line by means of an established technique[11] and HARP by 2 independent observers. Coordinates of the posterior right ventricular–LV insertion point were calculated on the most basal slice and were used as reference landmarks for segmentation of the LV. The myocardium was divided into 5 segments as follows: segment 1, inferior; 2, inferolateral; 3, lateral; 4, anterior; and 5, septal wall. For the conventional analysis, images were processed with the use of an in-house–developed software program (Findtags). This method requires interactive and time-consuming detection of myocardial contours and tag lines and generates a detailed motion map through the use of interpolation.[11] Detection of myocardial contours or tag lines was not necessary with HARP. Strain was defined as the deformation gradient and was related to the derivative of the phase, that is, the local frequency. Eulerian strain was calculated by means of the single-shot harmonic phase (SHARP) approach.[14] Three circles then were superimposed on the first image from the subendocardium, throughout the myocardium, to the subepicardium. The inner circle was placed as close as possible to the endocardium while avoiding papillary muscles. The outer circle was located as close as possible to the epicardium and the mid-circle, equally spaced between the inner and outer ones

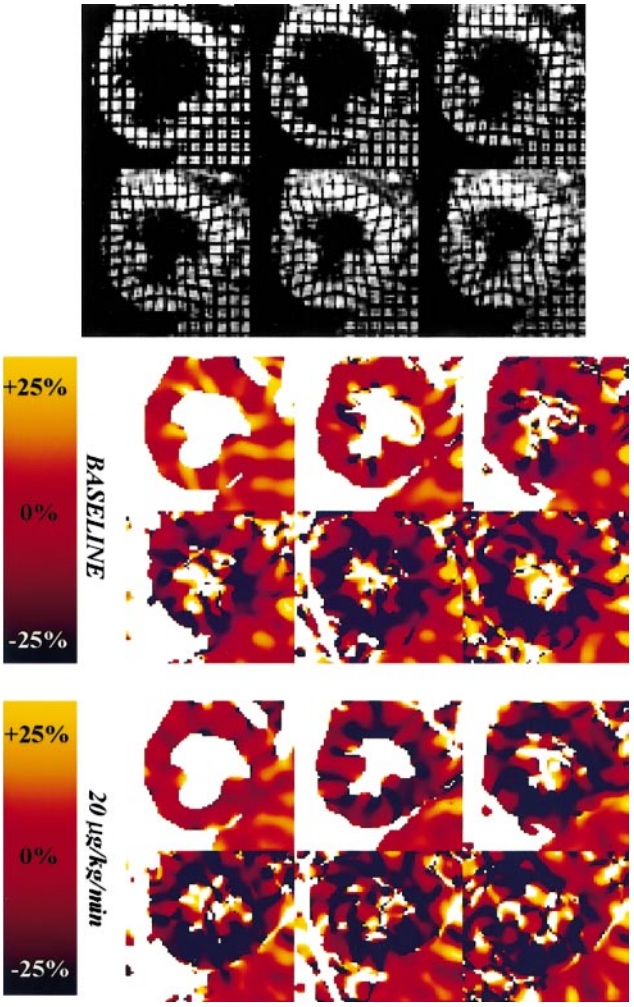

Figure 2. SPAMM-tagged images of the LV short-axis view throughout systole in a healthy volunteer at baseline (top) and the corresponding 2D strain maps by HARP (circumferential shortening) with 5 (middle) and 20 $\mu g^{-1} \cdot kg^{-1} \cdot min^{-1}$ (bottom) dobutamine. Black indicates shortening; yellow indicates stretching. HARP allowed strain to be calculated at any arbitrary pixel within the myocardium.

(Figure 3). For a single slice, 45 points (5 segments×3 layers×3 points per segment) were automatically tracked throughout systole by the cine-HARP approach.[16] Strain changes were assessed between the reference and the deformed state (end-systole) by the fractional changes in length in the circumferential direction (Ecc) in each myocardial layer. A negative value stands for compression of a line segment between 2 material points. In addition, we calculated maximal shortening (E_2) as a principal strain given by the magnitude as well as the direction of the associated eigenvector.

Myocardial wall thickening (MWT) measured from cine-MR images was used as a gold standard for the detection of regional wall motion abnormality in patients with coronary artery disease (CAD). It was calculated at baseline in postinfarct patients and volunteers (control group), in the entire LV, by use of the automatic detection of endocardial and epicardial boundaries (Findtags),[11] as

$$\mathrm{MWT}(\%)=\frac{\mathrm{EDWT}-\mathrm{EDWT}}{\mathrm{EDWT}}$$

where ESWT is end-systolic wall thickness and EDWT end-diastolic wall thickness. Wall motion abnormality (dysfunctional segments) was defined as a value of MWT <2 SD of the mean value in the control population and akinetic segments as segments with a MWT <5%.

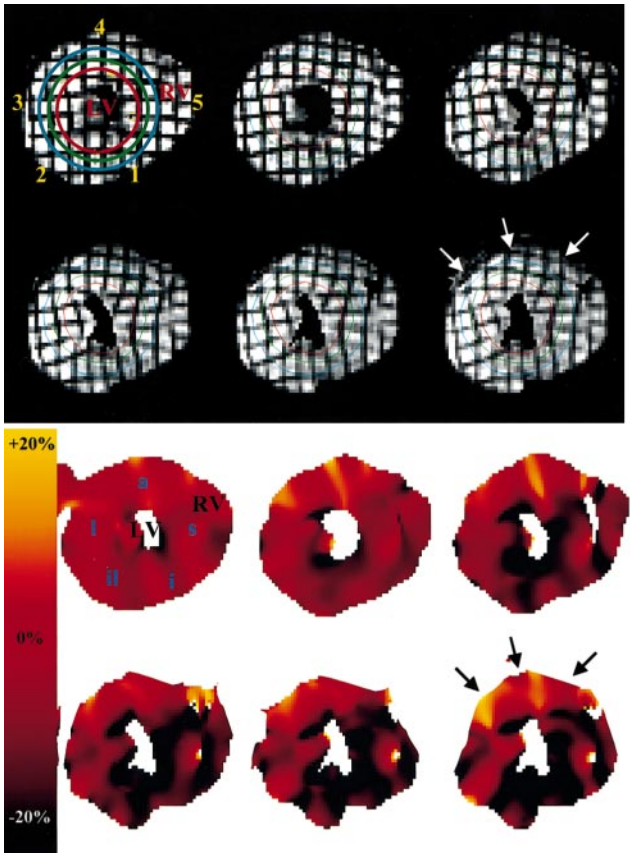

Figure 3. Segmentation of the myocardium by the use of 3 equally spaced circles (each divided into 5 segments) throughout the wall. Top, a sequence of LV tagged images throughout systole is displayed in a patient with a recent anterior AMI (arrows). The corresponding 2D map of circumferential shortening is shown at the bottom. RV indicates right ventricle; LV, left ventricle; s, septum; i, inferior; il, inferolateral; l, lateral; and a, anterior wall.

Statistical Analysis

Mean values are expressed as mean±SD. Comparisons between both methods were assessed by linear regression analysis and Bland-Altman plots. Mean values of myocardial strains in each myocardial layer were compared by paired Student's *t* test. Comparisons of myocardial strains under different doses of dobutamine were assessed by repeated-measures ANOVA. Percent increase in strain under dobutamine was compared by χ^2 analysis. Interobserver reproducibility of measurements by HARP was assessed in 4 randomly selected volunteers and 4 patients by the use of a linear regression analysis and by calculating the mean difference between both series of measurements. All tests were 2-tailed, and a value of $P<0.05$ was considered statistically significant.

Results

Myocardial Strain by HARP and Conventional Method

Once the filter specifications are defined for each series of images, full quantitative assessment of myocardial strains in a single slice took <3 minutes by HARP. Quantitative analysis of a complete data set (baseline and 2 steps of dobutamine) required ≈10 hours by the conventional approach and 60 minutes by HARP. For pooled data in normal and dysfunctional myocardium, HARP led to reproducible results between 2 independent observers for Ecc, E_2, and E_2 direction. Regression

coefficients between both analyses were $r=0.98$, 0.99, and 0.97, respectively ($P<0.0001$). Mean differences between both analyses were $5.4\times10^{-4}\pm3.5\times10^{-3}$ (<2%), $1.8\times10^{-3}\pm9.6\times10^{-3}$ (<2%), and 1.2±2.7° (<4%), respectively (NS).

For pooled data from volunteers and patients, the 2 methods showed good correlation. For Ecc, E_2, and E_2 direction, regression coefficients were $r=0.93$ ($P<0.001$) (Figure 4). Comparisons between data are displayed in Bland-Altman plots in Figure 5. In volunteers, the mean differences between both techniques were $1.1\times10^{-3}\pm2.6\times10^{-2}$ (0.5%, NS), $3.6\times10^{-3}\pm2.1\times10^{-2}$ (1.6%, $P<0.01$), and 1.1±4.1° (7%, $P<0.01$), for each strain, respectively. HARP led to a slight underestimation of each myocardial strain in the subendocardium (−0.231±0.042 vs −0.236±0.050, $P=0.008$, −0.256±0.049 vs −0.262±0.056, $P<0.0001$, and 15.6±6.4 vs 17.3±6.6°, $P<0.0001$, respectively). In patients with CAD, the mean differences between both methods were also very small and statistically not significant ($5.1\times10^{-3}\pm3.4\times10^{-2}$, $4.1\times10^{-3}\pm3.5\times10^{-2}$, and 0.2±6.2°, respectively).

Myocardial Strain Changes Induced by Dobutamine

The mean time in the magnet was ≈30 minutes. We did not observe any significant side effect during dobutamine infusion. The evolution of 2D strains under dobutamine is displayed in Figure 6. For each strain, both techniques were able to detect a transmural strain gradient. Recruitable myocardial strain (%Δ increase at peak dobutamine) as assessed by HARP increased similarly in subendocardium and subepicardium (22.4% vs 21.6% for Ecc and 27.2% vs 26.5% for E_2, P=NS). The 2 methods were able to depict subtle changes in myocardial strains during dobutamine stimulation (5 $\mu g^{-1}\cdot kg^{-1}\cdot min^{-1}$ vs baseline, $P<0.01$, and 20 vs 5 $\mu g^{-1}\cdot kg^{-1}\cdot min^{-1}$, $P<0.001$). E_2 orientation shifted further from the circumferential direction at 20 $\mu g^{-1}\cdot kg^{-1}\cdot min^{-1}$ as compared with baseline (18±6° vs 12±5°, $P<0.01$) (Figure 6). At baseline, Ecc and E_2 were greater in LV free wall (ie, lateral and posterolateral wall) than in the septum ($P<0.01$) (Table). However, recruitable strain at peak dobutamine was greater in LV septum than in free wall (24.1% vs 14.6% and 27.6% vs 16.1%, for Ecc and E_2, respectively, $P<0.01$). At baseline, Ecc and E_2 were greater at the apex compared with the base ($P<0.01$) (Table), but recruitable deformation was not significantly different at the apex versus the base (21.2% vs 19.8% and 21.2% vs 19.7%, respectively, NS).

Myocardial Strain in Patients With CAD

Myocardial strain was measured in 9 patients (8 men, 43±11 years) at baseline, 3±2 days after a first AMI (4 anterior, 5 inferior), and compared with MWT obtained from cine-MR images. Of the 180 segments analyzed (5 segments×4 slices×9 patients), 98 were classified as dysfunctional according to wall thickening analysis (ie, MWT <2 SD). Of these, 46 were classified as akinetic (MWT <5%). Figure 3 shows an example of a strain map obtained by HARP in a patient with anterior AMI. In each layer, Ecc and E_2 were decreased in dysfunctional myocardial segments when compared with remote ($P<0.001$) and further decreased in akinetic segments ($P<0.01$ vs dysfunctional) (Figure 7). E_2 direction was increased in dysfunctional segments when compared with remote (34±19 vs 19±10°, in the subendocardium, $P<0.001$) and was further augmented in akinetic segments (41±21°, $P<0.01$ vs dysfunctional).

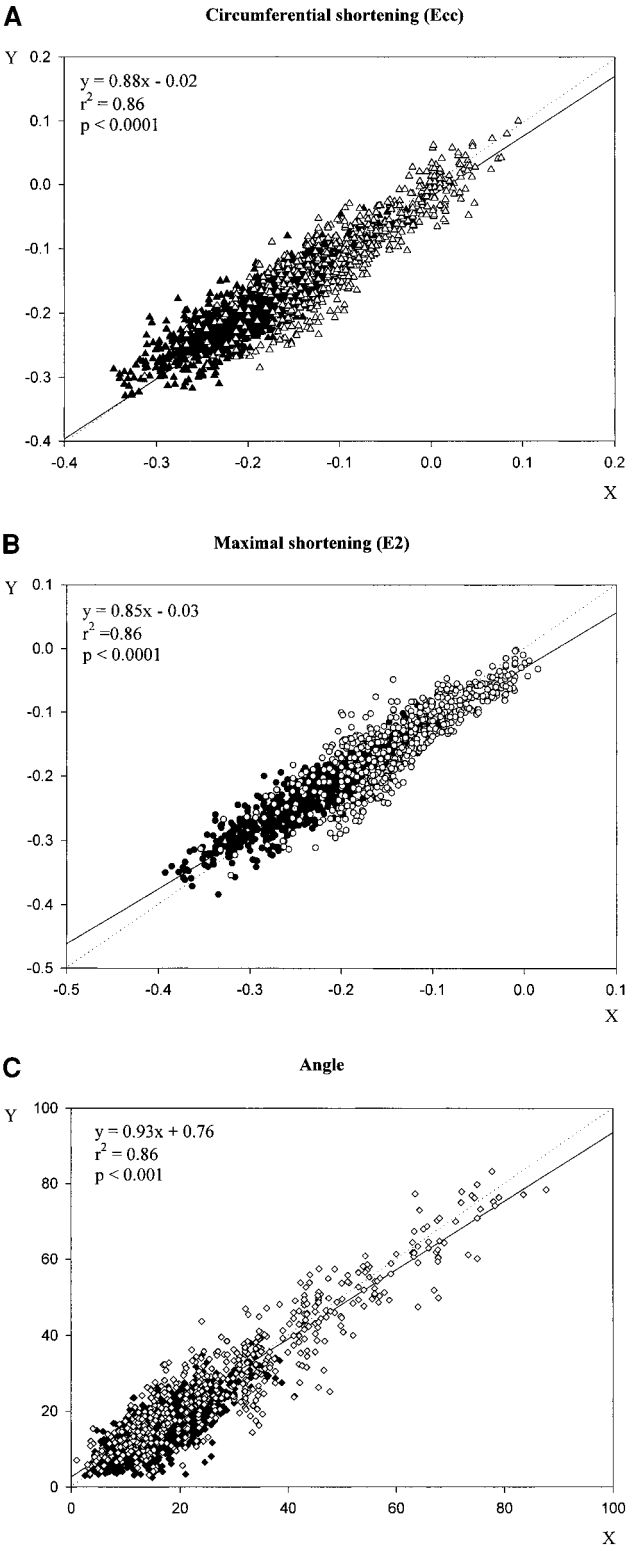

Figure 4. Correlation between myocardial strain as assessed by HARP (*y*-axis) and the conventional method (*x*-axis) for Ecc (A), E_2 (B), and E_2 direction (C). Black symbols indicate volunteers; white symbols, patients with CAD.

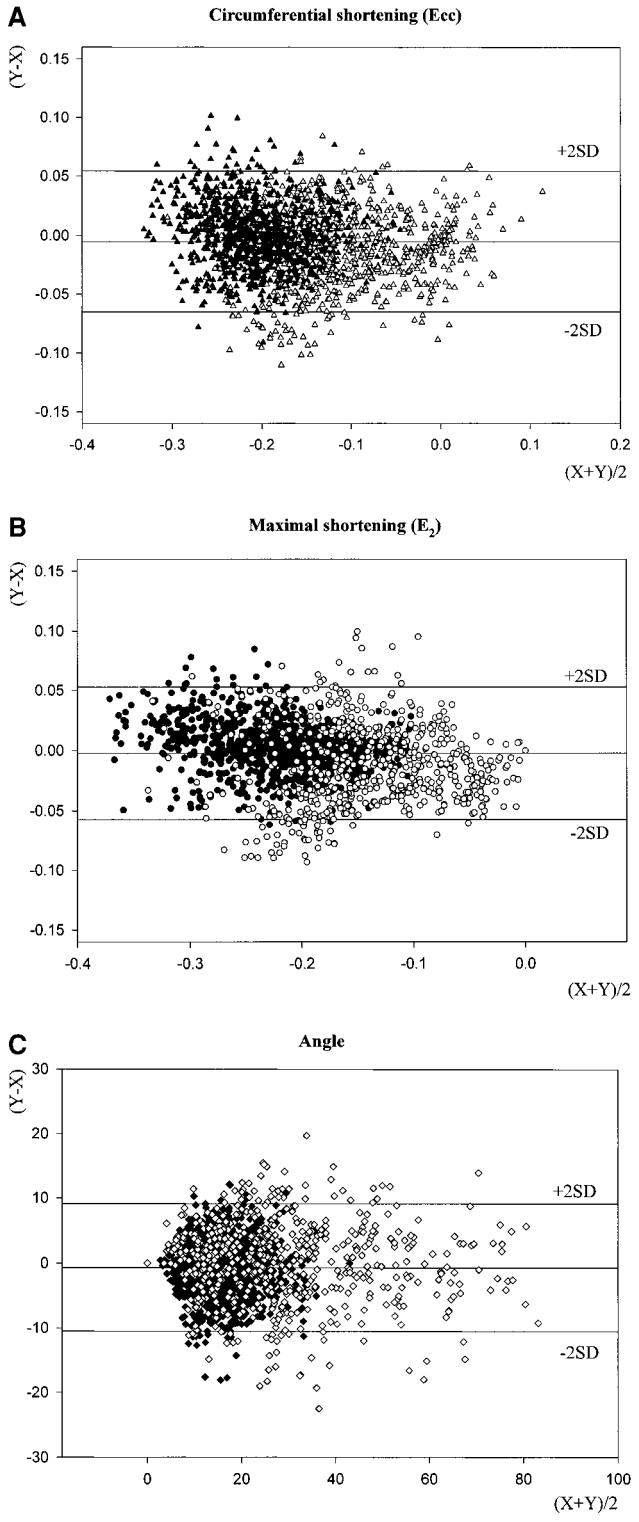

Figure 5. Bland-Altman plots for the comparison of myocardial circumferential shortening (A), maximal shortening (B), and the direction of the eigenvector (C). Black symbols indicate volunteers; white symbols, patients with CAD.

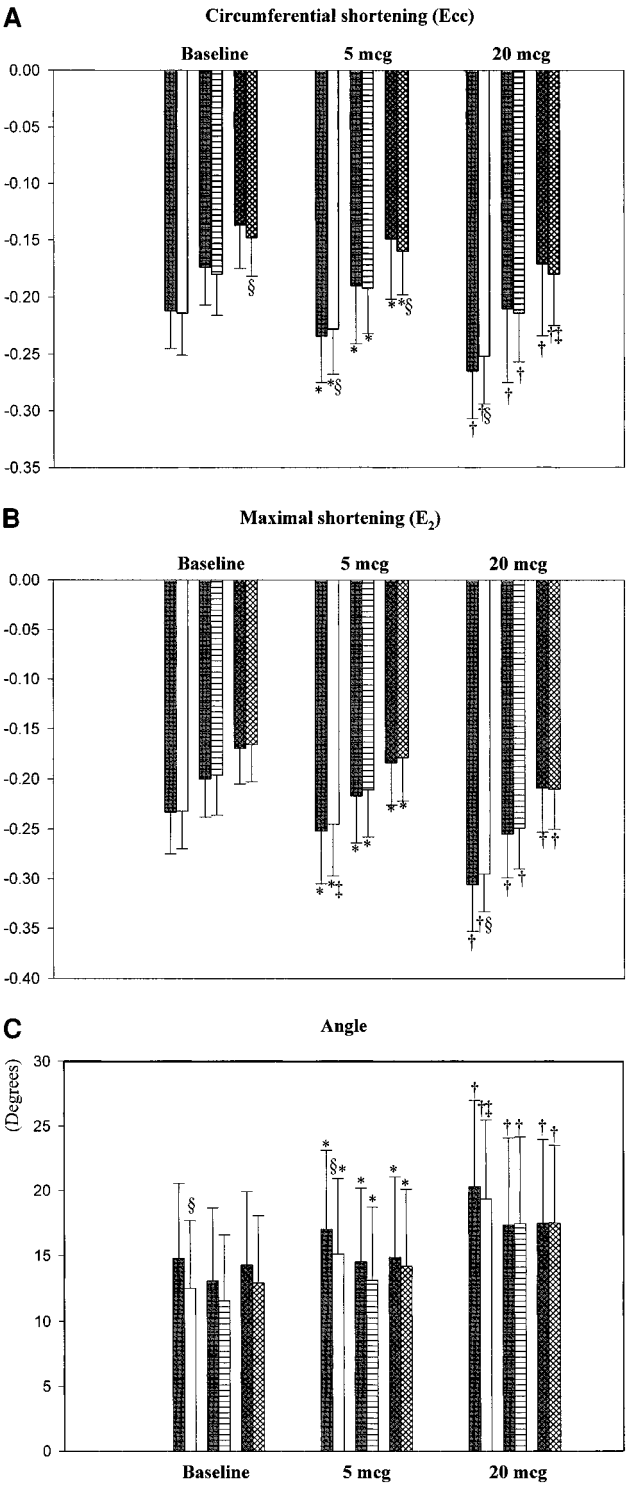

Figure 6. Evolution of circumferential shortening (A), maximal shortening (B), and the direction of the eigenvector (C) as assessed by the conventional technique (gray bars) and by HARP (white bars) in the subendocardium (solid bars), midwall (striped bars), and subepicardium (hatched bars) at baseline and under increasing doses of dobutamine. *$P<0.01$ vs baseline, †$P<0.001$ vs 5 $\mu g^{-1} \cdot kg^{-1} \cdot min^{-1}$ dobutamine. ‡$P<0.05$ and §$P<0.01$ vs conventional technique.

Discussion

We describe and validate a new image processing method (HARP) based on the use of isolated spectral peaks in SPAMM-tagged MR images, which allows for rapid analysis of myocardial strain from tagged cardiac images. We also use MRI tagging to measure the effect of graded dobutamine stimulation on regional myocardial mechanics in the normal human LV. HARP is based on the fact that the inverse Fourier transform of a spectral peak in the Fourier domain is a

Dobutamine-Induced Modifications of Circumferential (Ecc) and Maximal Shortening (E_2) Analyzed Segment by Segment and at Each Level in the Left Ventricle

	Ecc			E_2		
	Baseline	5 μg	20 μg	Baseline	5 μg	20 μg
By segment						
Posterior	−0.1760±0.0486*	−0.1854±0.0512	−0.2153±0.0572†	−0.1817±0.0411*	−0.1932±0.0504	−0.2319±0.0672†
Posterolateral	−0.2016±0.0383	−0.2100±0.0426	−0.2261±0.0456	−0.2208±0.0396	−0.2394±0.0473	−0.2589±0.0599
Lateral	−0.1979±0.0373	−0.2098±0.0387	−0.2313±0.0474	−0.2131±0.0419	−0.2255±0.0495	−0.2447±0.0581
Anterior	−0.1739±0.0432*	−0.1943±0.0468	−0.2113±0.0519†	−0.1925±0.0458*	−0.2010±0.0534	−0.2335±0.0546†
Septal	−0.1545±0.0377*	−0.1666±0.0464	−0.1917±0.0500†	−0.1600±0.0411*	−0.1720±0.0473	−0.2060±0.0553†
By level						
Base	−0.1711±0.0481	−0.1848±0.0541	−0.2050±0.0571	−0.1841±0.0496	−0.1987±0.0610	−0.2204±0.0652
Middle	−0.1844±0.0442	−0.1961±0.0437	−0.2143±0.0485	−0.1923±0.0434	−0.2013±0.0483	−0.2286±0.0547
Apex	−0.1869±0.0398‡	−0.2008±0.0448‡	−0.2266±0.0484‡	−0.2115±0.0410‡	−0.2200±0.0538‡	−0.2564±0.0587‡

Myocardial strain was obtained by averaging values of strains throughout the wall. Strain at mid-LV was obtained by calculating the average strain from the 2 mid-slices.

*$P<0.01$ vs free wall (posterolateral and lateral), †$P<0.01$ for %Δ increase vs LV free wall, and ‡$P<0.01$ vs base.

complex image with phase linearly related to a directional component of tissue displacement. This permits the isolation of tag motion components, making the analysis of regional function completely automatic. We demonstrate that measurements of 2D myocardial strains by HARP are reproducible and similar to those obtained by a conventional tag motion tracking technique, both in patients with CAD with wall motion abnormalities and in normal volunteers at rest and during inotropic stimulation.

Dobutamine-Induced Myocardial Strain Alterations in the Normal Human Heart

Previous studies using tagged MRI have reported normal values and regional variations in 2D systolic strains at rest.[17,18] We compared myocardial deformation at 20 $\mu g^{-1} \cdot kg^{-1} \cdot min^{-1}$ versus baseline and found a significant increase in both circumferential and maximal shortening. Other studies focusing on the effect of dobutamine on regional LV function as assessed by tagged MRI in normal subjects have shown an increase in myocardial strain from baseline to 10 $\mu g^{-1} \cdot kg^{-1} \cdot min^{-1}$ and no dobutamine-induced wall motion heterogeneity.[19,20] Our data confirm that dobutamine does not further exacerbate variations in regional wall motion contractility documented at rest. Although Ecc and E_2 were less in the anteroseptal than in the LV free wall at baseline, percent increase in myocardial strain under dobutamine was greater in the anteroseptal than in the free wall, resulting in a relative homogeneity of myocardial contraction under inotropic stimulation. When analyzed by cross-sectional level along the LV long axis, dobutamine infusion resulted in a uniform increase in myocardial strains, in agreement with recently reported data.[20]

Because of wall shear (differences between subepicardial and subendocardial rotational deformation), maximal shortening does not occur in the same direction as circumferential shortening (Figure 8). We report a slight increase in the angle between Ecc and E_2 orientations as a result of dobutamine stimulation, indicating that dobutamine slightly amplifies myocardial wall shear. In agreement with previous studies,[20] the angle remained <20°, indicating that maximal shortening still remained circumferentially oriented. Previous work has shown that dobutamine leads to increased rotation of both subepicardial and subendocardial layers in the normal left ventricle.[21] Because rotation increases in both layers, changes in the direction of the eigenvector are blunted, maintaining LV efficiency.

Potential Advantages of HARP

HARP can be used with any tagging technique provided the tag pattern is planar and tag lines are uniformly apart from each other. We assessed myocardial strain off-line from the tagged-image data set. We defined the filter specifications for each series of images, which represents the most time-consuming part before the HARP analysis (30 to 40 minutes). Once the filter is set, a full quantitative analysis of the data typically takes <3 minutes. Standardized acquisitions of tagged images allow subsequent presetting of the filter and can provide very fast myocardial strain mapping. Furthermore, HARP images can be extracted directly from the raw data, allowing very fast display of 2D strain fields. In other words, HARP may provide on-line detailed quantitative assessment of 2D myocardial strains.

Future Clinical Applications

HARP may have important clinical applications by overcoming the main limitation to routine clinical utilization of tagged cardiac MRI. When used in combination with dobutamine-tagged MRI, HARP might be of great value for the detection of myocardial ischemia during stress testing. Similarly, it might provide fast and accurate quantification of functional recovery in stunned or hibernating but viable myocardium.[22,23] It also might be useful for studying dynamic changes in regional LV function after acute infarction by allowing serial quantitative examinations over time.[24,25] Alterations in LV torsional deformation may be important in several pathological states.[26] Because HARP has the potential for other applications of any tracking motion technique, it allows for rapid noninvasive assessment of twist mechanics in the human heart, in different myocardial segments, and at each myocardial layer.

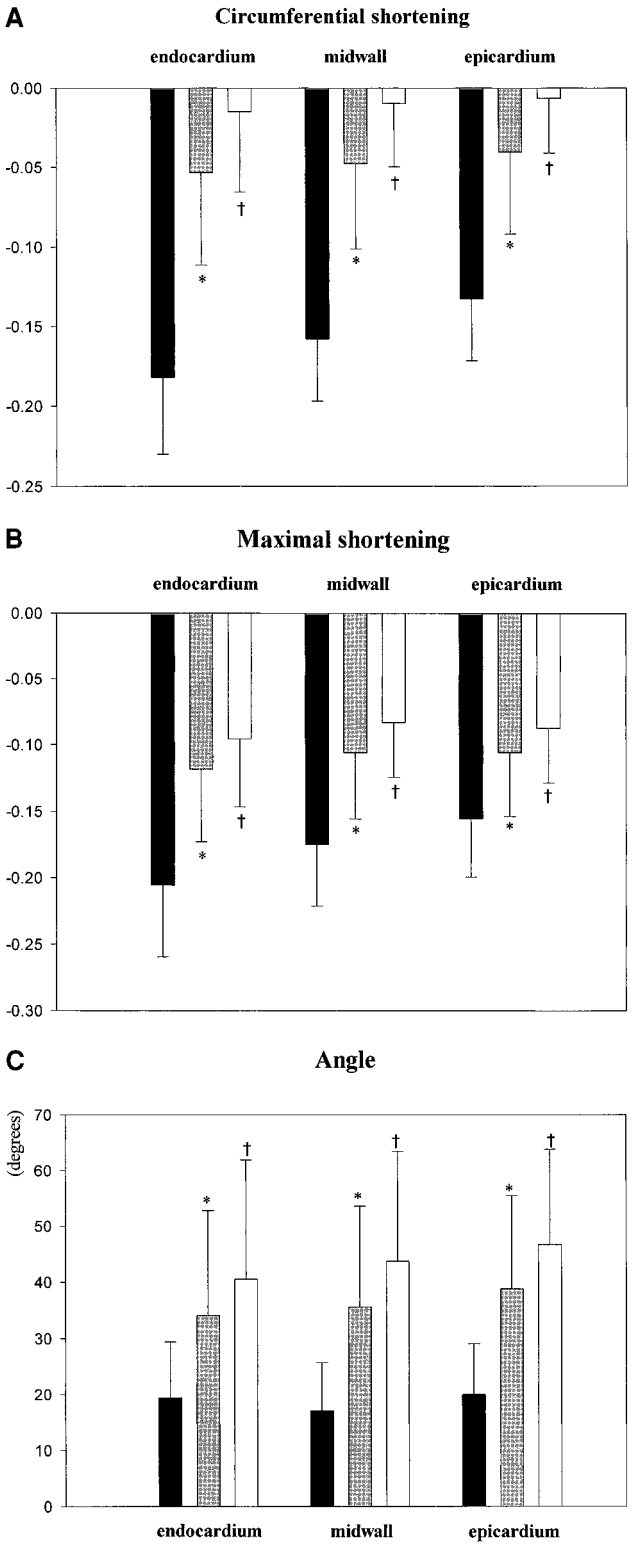

Figure 7. Ecc (A), E_2 (B), and E_2 direction (C) in dysfunctional (hypo+akinetic; gray bars) and akinetic segments (white bars) in patients with CAD. *$P<0.001$ vs remote (black bars), †$P<0.01$ vs dysfunctional.

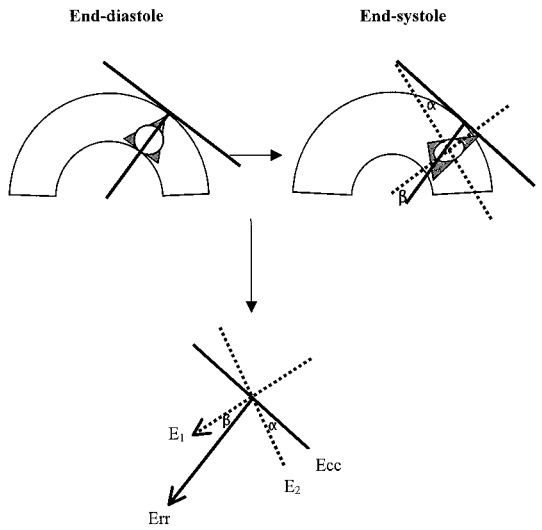

Figure 8. Schematic representation of LV short-axis slice. Systolic deformation of a triangle and a circle located within the myocardium is shown. The direction of the normal circumferential strain (Ecc) is parallel to the tangent of the myocardium in respect to the heart surface. The direction of the normal radial strain (Err) is perpendicular to the circumferential direction, toward the ventricular centroid. Because of wall shear, a circle would be deformed into an ellipse during systole. Principal strains are given by the magnitude and direction of the eigenvector. The major and minor axes of the ellipse are representations of the minimal principal strain (maximal shortening, E_2) and the greatest principal strain (maximal elongation, E_1). In addition to the magnitude of E_2 and Ecc, we assessed angle α between the direction of Ecc and that of E_2.

Study Limitations

We measured 2D myocardial strain fields and did not compensate for through-plane translation of the heart.[27,28] It is known that 3D deformation allows more accurate evaluation of cardiac mechanics.[29] However, 2D analysis of regional myocardial function by tissue tagging is sufficiently powerful surements of small planar displacements by HARP are readily extendable to 3D motion by use of the out-of-plane tag direction for quantitative assessment of a 3D strain tensor.[14,16]

Conclusions

HARP MRI provides fast, accurate measurements of 2D strain fields from tagged MR images in normal individuals and in patients with wall motion abnormalities caused by CAD. It allows for detailed analysis of the effect of graded dobutamine stimulation on regional myocardial mechanics in the normal human LV. Finally, with standardized acquisitions, HARP has the potential for providing on-line quantitative monitoring of LV function during stress testing in humans.

Appendix A

Harmonic Images

Let $y \epsilon R^2$ represent the coordinates of a point in the imaging plane. The intensity of this point at time t is given by the scalar quantity $I(y, t)$. The tagged image can be written as

$$I(y, t) = I^o(y, t)\, f(y, t)$$

where I^o represents the image without tag lines and f is a periodic function describing the tag pattern. We can use the Fourier series to expand the SPAMM-tag pattern into a harmonic summation, as

$$I(y, t) = \sum_{k=0}^{K-1} I_k(y, t)$$

where K depends on the tag pattern specifications. Each term I_k is a complex image corresponding to a harmonic image. A harmonic image is given by a magnitude D_k and a phase ϕ_k as

$$I_k(y, t) \triangleq D_k(y, t) e^{j\phi_k(y,t)}$$

with

$$\phi_k(y, t) = \omega_k^T q(y, t)$$

where ω_k is the tag frequency vector of the corresponding harmonic peak. The phase is related to the motion according to the reference mapping function $q(y, t)$ that maps any point at (y, t) into its reference location q when the tag pattern was imposed.

Wrapping Artifact

We obtained a wrapped version of the phase corresponding to the harmonic phase image a_k. HARP images are related to the actual phase ϕ_k

$$a_k = W[\phi_k]$$

where W is the nonlinear wrapping function given by

$$W(\phi) = \mathrm{mod}(\phi + \pi, 2\pi) - \pi$$

Appendix B

The Eulerian strain is related to the difference in displacement between adjacent parts of the myocardium. It can be computed from 2 HARP images (a_1 and a_2) having 2 linearly independent vectors ω_1 and ω_2. The apparent strain in the direction e is given by

$$\epsilon_a(y, t; e) = \left\| \begin{bmatrix} \nabla_y^* a_1(y, t) \\ \nabla_y^* a_2(y, t) \end{bmatrix}^{-1} \Omega^T e \right\| - 1$$

where

$$\nabla_y^* a_k = \begin{cases} \nabla_y a_k & \|\nabla_y a_k\| \le \|\nabla_y a_k^{(\pi)}\| \\ \nabla_y a_k^{(\pi)} & \text{otherwise} \end{cases}$$

the matrix $\Omega \epsilon R^{2\times 2} = [\omega_1 \omega_2]$

and

$$a_k^{(\pi)}(y, t) \equiv W(a(y, t) + \pi)$$

for k=1,2.

Acknowledgments

This work was supported by NIH/NHLBI grants R29HL-47405 and HL-45090 and by grant NO1-HC95162. Dr Garot was supported by the Institut Roche Cardiovasculaire (Paris, France). The authors thank T. Faranesh for the development of the pulse sequence and conventional strain analysis software.

References

1. Marwick TH. Current status of stress echocardiography for diagnosis and prognostic assessment of coronary artery disease. *Coron Artery Dis*. 1998;9:411–426.
2. Nagel E, Lehmkuhl HB, Bocksch W, Klein C, Vogel U, Frantz E, Ellmer A, Dreysse E, Fleck E. Noninvasive diagnosis of ischemia-induced wall motion abnormalities with the use of high-dose dobutamine stress magnetic resonance imaging: comparison with dobutamine stress echocardiography. *Circulation*. 1999;99:763–770.
3. Picano E, Lattanzi F, Orlandini A, Marini C, L'Abbate A. Stress echocardiography and the human factor: importance of being expert. *J Am Coll Cardiol*. 1991;17:666–669.
4. Zerhouni EA, Parish DM, Rogers WJ, Yang A, Shapiro EP. Human heart: tagging with MR imaging: a method for noninvasive assessment of myocardial motion. *Radiology*. 1988;169:59–63.
5. Young AA, Axel L. Three-dimensional motion and deformation of the heart wall: estimation with spatial modulation of magnetization: a model-based approach. *Radiology*. 1992;185:241–247.
6. O'Dell WG, Moore CC, Hunter WC, Zerhouni EA, McVeigh ER. Three-dimensional myocardial deformations calculation with displacement field fitting to tagged MR images. *Radiology*. 1995;195:829–835.
7. Axel L, Dougherty L. MR imaging of motion with spatial modulation of magnetization. *Radiology*. 1989;171:841–845.
8. Axel L, Dougherty L. Heart wall motion: improved method of spatial modulation of magnetization for MR imaging. *Radiology*. 1989;172:349–350.
9. Denney TS Jr, Prince JL. Reconstruction of 3D left ventricular motion from planar tagged cardiac MR images: an estimation theoretic approach. *IEEE Trans Med Imaging*. 1995;14:625–635.
10. Young AA, Kraitchman DL, Dougherty L, Axel L. Tracking and finite element analysis of stripe deformation in magnetic resonance tagging. *IEEE Trans Med Imaging*. 1995;14:413–421.
11. Guttman M, Prince JL, McVeigh ER. Tag and contour detection in tagged cardiac magnetic resonance images of the left ventricle. *IEEE Trans Med Imaging*. 1994;13:74–88.
12. Moore CC, Reeder SB, McVeigh ER. Tagged MR imaging in a deforming phantom: photographic validation. *Radiology*. 1994;190:765–769.
13. Guttman MA, Zerhouni EA, McVeigh ER. Analysis and visualization of cardiac function from MR images. *IEEE Comp Graph Appl*. 1997;17:30–38.
14. Osman NF, Prince JL. Angle images for measuring heart motion from tagged MRI. *Proc IEEE Conf Image Proc*. 1998;I:704–708.
15. McVeigh ER, Atalar E. Cardiac tagging with breath-hold cine MRI. *Magn Reson Med*. 1992;28:318–327.
16. Osman NF, Faranesh AZ, McVeigh ER, Prince JL. Tracking cardiac motion using cine harmonic phase (HARP) magnetic resonance imaging. *Proc Int Soc Magn Reson Med*. 1999;22–28.
17. Young AA, Imai H, Chang CN, Axel L. Two-dimensional left ventricular deformation during systole using magnetic resonance imaging with a spatial modulation of magnetization. *Circulation*. 1994;89:740–752.
18. Clark NR, Reichek N, Bergey P, Hoffman EA, Brownson D, Palmon L, Axel L. Circumferential myocardial shortening in the normal human left ventricle: assessment by magnetic resonance imaging using spatial modulation of magnetization. *Circulation*. 1991;84:67–74.
19. Power TP, Kramer CM, Shaffer AL, Theobald TM, Petruolo S, Reichek N, Rogers WJ Jr. Breath-hold dobutamine magnetic resonance myocardial tagging: normal left ventricular response. *Am J Cardiol*. 1997;80:1203–1207.
20. Scott CH, Sutton MS, Gusani N, Fayad Z, Kraitchman D, Keane MG, Axel L, Ferrari VA. Effect of dobutamine on regional left ventricular function measured by tagged magnetic resonance imaging in normal subjects. *Am J Cardiol*. 1999;83:412–417.
21. Buchalter MB, Weiss JL, Rogers WJ, Zerhouni EA, Weisfeldt ML, Beyar R, Shapiro EP. Noninvasive quantification of left ventricular rotational deformation in normal humans using magnetic resonance imaging myocardial tagging. *Circulation*. 1990;81:1236–1244.
22. Geskin G, Kramer CM, Rogers WJ, Theobald TM, Pakstis D, Hu YL, Reichek N. Quantitative assessment of myocardial viability after infarction by dobutamine magnetic resonance tagging. *Circulation*. 1998;98:217–223.
23. Baer FM, Theissen P, Schneider CA, Voth E, Sechtem U, Schicha H, Erdmann E. Dobutamine magnetic resonance imaging predicts contractile recovery of chronically dysfunctional myocardium after successful revascularization. *J Am Coll Cardiol*. 1998;31:1040–1048.
24. Kramer CM, Lima JAC, Reichek N, Ferrari VA, Llaneras MR, Palmon LC, Yeh IT, Tallant B, Axel L. Regional differences in function within noninfarcted myocardium during left ventricular remodeling. *Circulation*. 1993;88:1279–1288.
25. Lima JAC, Ferrari VA, Reichek N, Kramer CM, Palmon L, Llaneras MR, Tallant B, Young AA, Axel L. Segmental motion and deformation of transmurally infarcted myocardium in acute postinfarct period. *Am J Physiol*. 1995;268:H1304–H1312.
26. Hansen DE, Daughters GT II, Alderman EL, Ingels NB Jr, Miller DC. Torsional deformation of the left ventricular midwall in human hearts with intramyocardial markers: regional heterogeneity and sensitivity to the inotropic effects of abrupt rate changes. *Circ Res*. 1988;62:941–952.
27. Rogers WJ Jr, Shapiro EP, Weiss JL, Buchalter MB, Rademakers FE, Weisfeldt ML, Zerhouni EA. Quantification of and correction for left ventricular systolic long-axis shortening by magnetic resonance tissue tagging and slice isolation. *Circulation*. 1991;84:721–731.
28. Stuber M, Scheidegger MB, Fischer SE, Nagel E, Steinemann F, Hess OM, Boesiger P. Alterations in the local myocardial motion pattern in patients suffering from pressure overload due to aortic stenosis. *Circulation*. 1999;100:361–368.
29. Lima JAC, Jeremy R, Guier W, Bouton S, Zerhouni EA, McVeigh ER, Buchalter MB, Weisfeldt ML, Shapiro EP, Weiss JL. Accurate systolic wall thickening by nuclear magnetic resonance imaging with tissue tagging: correlation with sonomicrometers in normal and ischemic myocardium. *J Am Coll Cardiol*. 1993;21:1741–1751.

Fast Determination of Regional Myocardial Strain Fields From Tagged Cardiac Images Using Harmonic Phase MRI

Jérôme Garot, David A. Bluemke, Nael F. Osman, Carlos E. Rochitte, Elliot R. McVeigh, Elias A. Zerhouni, Jerry L. Prince and João A. C. Lima

Circulation. 2000;101:981-988
doi: 10.1161/01.CIR.101.9.981
Circulation is published by the American Heart Association, 7272 Greenville Avenue, Dallas, TX 75231

Print ISSN: 0009-7322. Online ISSN: 1524-4539